2021 IEEE/SICE International Symposium on System Integrations (SII)
Iwaki, Fukushima, Japan. January 11 - 14, 2021

Evaluation of mapping and path planning for non-holonomic mobile robot navigation in narrow pathway for agricultural application

Anupam Choudhary[1] Yuichi Kobayashi[1] Francisco J. Arjonilla[2] Satoshi Nagasaka[3] Megumu Koike[3]

Abstract— **This paper evaluates mapping and path planning methods for mobile robot with non-holonomic constraint in the narrow pathways. Selection of sensors such as depth camera or LiDAR sensor is complex problem as it depends on applications, demand for cost, robustness and data processing. Along with sensor selection map generation is essential task for mobile robot navigation. This paper presents experimental evaluation of laser-based mapping algorithm *i.e.*, Gmapping and vision based mapping *i.e.*, RTAB-Map. The platform used for autonomous navigation is mobile robot with non-holonomic constraint. The path planning for mobile robot with non-holonomic constraint is more complex as not all arbitrary trajectories are kinematically feasible. The application of mobile robot navigation is to transfer agriculture products in greenhouse from one place to another. Generally, the pathways of greenhouse are narrow, which often results in the planner failing to generate a traversable trajectory if the mobile robot is restricted to forward movement, hence the switch-back (forward and backward) path planning is essential to navigate in such environments. In the following discussion, we implement the Reeds-Shepp curve based path planning for mobile robot with a non-holonomic constraint to navigate in narrow pathways. Reeds-Shepp curve can generate various combinations of such switch-back trajectories and it remains unmatched in terms of computation efficiency and reliability compared to other curves. Effectiveness of the proposed path planning method is validated experimentally.**

I. Introduction

Over the last two decades, the amount of research activities in the field of mobile robot has increased rapidly, especially in agricultural environments. Green houses are known as an example of agricultural environment and they have narrow pathways, where planning methods have been widely investigated [1], [2]. The application of mobile robots with holonomic constraints such as omnidirectional robots are limited to transfer light load and are more expensive. In agricultural fields and in greenhouses, it is required to carry heavy loads in dirty and often muddy environments, which makes the use of omnidirectional wheels infeasible.

Furthermore, agricultural environments are complex with many sources of uncertainty such as unreliable readings of distance to vegetation and unreliable dead-reckoning. Even so, accurate mapping is necessary for effective navigation in these environments. In the green house environment, there have been several implementations of mobile robots [3], [4], [5]. But as far as we know, there have been no experimental comparisons between the existent mapping methods in agricultural scenarios. In this paper, we experimentally evaluate a grid-based 2D mapping method [6] in the implementation provided by ROS as *GMapping* [7] and a 3D mapping method *RTAB-Map* [8] on the basis of quality and update frequency of the grid maps produced, which is the first contribution.

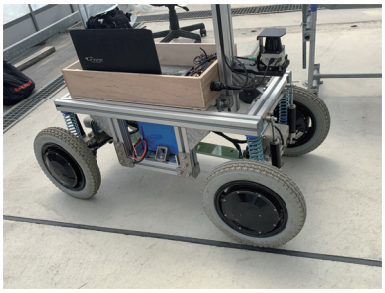

Fig. 1: A four-wheeled mobile robot with non-holonomic constraint

Path planning for mobile robot with non-holonomic constraints is a complex problem because not every trajectory is kinematically feasible. Common path planning algorithms for narrow spaces include probabilistic road map (PRM) [9], extended spatial tree (EST), and rapid search random tree (RRT*) [10]. One of the approaches to planning non-holonomic mobile robot trajectory is to apply Reeds-Shepp curve [11], which is known as combinations of circular and linear trajectories allowing switching back motion.

Integrating Reeds-Shepp curve to planning algorithm has been proposed in [12] with RRT algorithm for parking problem [1]. In this paper, we implement and evaluate combination of Reed-Shepp curve and RRT* planning algorithm on a four-wheeled mobile robot in greenhouse environment. The second contribution of the paper is to evaluate the planning approach based on Reeds-Shepp curve in the greenhouse environment to obtain suggestions for more practical use.

II. Problem Definition

A four-wheel mobile robot with non-holonomic constraint is used as a platform for the experiment as shown in Figure 1. The mobile robot is equipped with four 250W hub motor and a 110Ah battery. The robot pose is uniquely described by $[x, y, \theta] \in \mathbb{R}^3$ where $[x, y, \theta]$ represents the coordinates and orientation of the mobile robot in the global frame. The

[1] Anupam Choudhary and Yuichi Kobayashi are with Faculty of Mechanical Engineering, Shizuoka University, Japan
[2] Francisco J. Arjonilla is with Graduate School of Science and Technology, Shizuoka University, Japan
[3] Satoshi Nagasaka and Megumu Koike are with Somic Management Holdings Inc., Japan.

[1] A ROS implementation of Reeds-Shepp curve exists in [13], but it is not combined with any planning algorithm.

TABLE I: Configuration parameters of the environment and the mobile robot

Width of pathways	0.60 m
Robot speed	2.5 m/sec
Mobile robot (l, b, h)	$100 \times 50 \times 50$
Robot minimum turning radius	0.35 m
Odometry sensor	depth camera (RealSense)
Vision sensor (obstacle detection)	2D LiDAR (Sick)
CPU of controller PC	2.9 Ghz Intel Core i7
Memory & Linux version	16 GByte, Ubuntu 16.04.7 LTS
Global path planning algorithm	RRT* and A*
Local path planning algorithm	E-band and DWA
localization algorithm	AMCL and RTAB-Map

Fig. 2: Navigational environment of the robot

problem of mapping and path planning can be defined in two statements.

1) The depth camera sensor and the laser scanner sensor from the viewpoint of computational time are evaluated. Also, their availability in agricultural environments is discussed.
2) The mobile robot navigation in narrow pathways, where forward-backward switching is required due to non-holonomic constraint is discussed. In this paper we implement Reeds-Shepp curve-based local path planning to adapt the middleware of ROS to such constrained mobile robot kinematics.

The mobile robot has double Ackerman steering system. The navigation environment is a greenhouse with narrow pathways surrounded by vegetation as shown in Figure 2. The parameters of mapping and navigation are defined in TABLE I. [2]

III. Evaluation of Robot Mapping and Localization

Implementation of navigation is based on the following two packages:

[2]The abbreviations in TABLE I are: AMCL, Adaptive Monte Carlo Localization; RRT*, Rapidly exploring random tree; DWA, Dynamic window approach.

- GMapping: For 2D mapping (SLAM), Rao-Blackwellized Particle Filtering [6] is implemented through GMapping, which is an open-source implementation of SLAM OpenSLAM. It creates a 2D occupancy grid map from laser scan data and the mobile robot pose. The sensor used for mapping are a Sick laser scanner for observation of 2D points and either a ZED stereo camera or a RealSense camera to obtain odometry (robot pose) information.
- RTAB-Map: For 3D mapping, RTAB-Map [14] is used. It can improve accuracy of the localization in agricultural environment with high vegetation conditions such as vegetables trees and vegetables leaves while it might take more computation in comparison with 2D mapping methods.

The two algorithms *i.e.*, Grid mapping and RTAB-Map generate an occupancy grid map. We evaluate whether the quality of the generated map is suited for mobile robot navigation.

A. Narrow pathways with fixed-height rack environment

In this environment, as shown in Figure 3, the navigation environment of the mobile robot has a narrow pathway and fixed rack on both sides of the pathways. The height of the plant is 0.60m from the ground and width of pathways is 0.75m.

It was verified that the GMapping generates a more reliable map in such environmental conditions. The mapping was evaluated by its robustness, map update rate and reliability. Sick LiDAR scanner (TIM781) was used for mapping and RealSense camera (D435) provided visual odometry information as its function. The parameter values used in our experiment is given in TABLE II.

The generated grid map with the top view of mapped environments is shown in Figure 4. It was confirmed that the Lidar-based SLAM (GMapping) reconstructed a more reliable map of the environment. Through totally 18 trials, the RTAB-Map failed from five to six times per trial to compute visual odometry estimation due to poor image feature detection. The map generated by RTAB-Map is shown in Figure 5.

Fig. 3: Fixed hight rack environment

TABLE II: Configuration parameters of localization by particle filter

Parameter	Value	Description
Particle	35	Number of particles in the filter
linearUpdate	1.2	Travelled distance for scan processing
linearUpdate	0.7	Rotated angle for scan processing
delta	0.04	Occupancy grid resolution (m)
occ-thresh	0.20	Threshold for occupied cell
iterations	6	The number of iterations

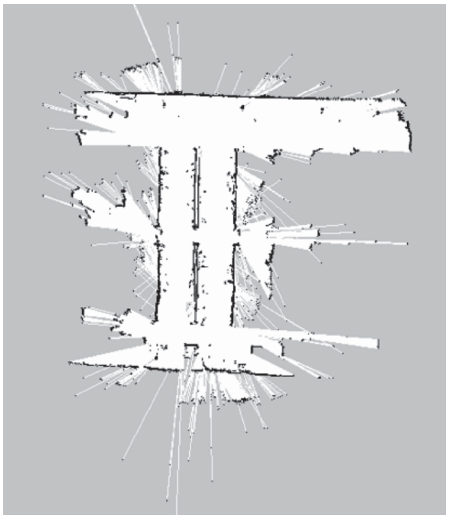

Fig. 4: Occupancy grid map generated by GMapping

B. Narrow pathways with natural obstacles of different height and density

In this environment, the pathways are surrounded by vegetation such as tomato plants and vines. Greenhouse features such as racks are hidden by the vegetation as shown in Figure 6. The average height of plants is approximately 1.5m and the pathway width is 0.75m. In the process of RTAB-Map, only RealSense camera information was used for both 3D map creation and visual odometry estimation inside the process. TABLE III [3] shows a list of relevant parameters and the values used in the experiments. RTAB-Map generates

TABLE III: Configuration parameters of map building

parameter	Value	Description
Grid/Cellsize	0.06	Occupancy grid resolution (m)
Mem/STMsize	12	Size of STM
Rtabmap/MemoryThr	0	Size of WM (0 = Inf.)
Rtabmap/DetectionRate	2	Detection rate (Hz)
Vis/FeatureType	6	Type of visual feature
Vis/Cortype	1	Feature matching

the occupancy grid map by computing 3D point clouds of the environment. During the mapping process, it was observed that the RTAB-Map often estimates incorrect robot poses. The robot pose was corrected by revisiting the same

[3]The abbreviation of mentioned terms in TABLE III are STM: Short term memory, WM: Working memory.

TABLE IV: Performance of mapping

Occupancy grid performance analysis - GMapping		
Sensor	Map quality	Map-update time (sec)
2D Lidar	High	0.0552
Occupancy grid performance analysis - RTAB-Map		
Sensor	Map quality	Map-update time (sec)
Depth camera	Good	0.0976

position multiple times. The mobile robot fails to recognise the position (x, y, θ) in 4 trails out of 10.

Figure 8 illustrates the occupancy grid map and Figure 7 illustrates the 3D point cloud of the environment from a third-person perspective. It was verified that the navigation environment has multiple pathways and the RTAB-Map could detect large loop closure effectively, given that miss-recognition of position can be avoided by multiple runs in the environment. Therefore, the generated grid map is reliable for navigation tasks.

C. Evaluation of computation time and discussion

TABLE IV depicts performance of RTAB-Map and GMapping in terms of map update frequency, sensor type, and map quality. The time in TABLE IV states the time required to update the 2D occupancy grid map. It was verified that the GMapping generates high quality map in fixed rack environments. In the fixed height rack environment, depth camera sensors failed to generate a map using GMapping due to irregular distribution of sunlight. And some of the invisible obstacles, which can be regarded as noise, were detected in the map. It also verified that the RTAB map generates good quality map in complex environment which is reliable for navigation but when compared with a frame rate of 20Hz in 2D LiDAR, observation update of RTAB-Map was around 10Hz, which limited navigation speed.

IV. Evaluation of Path Planning in Narrow Pathways

The aim of path planning techniques is to find the optimal path between $[x_i, y_i, \theta_i]$ and $[x_f, y_f, \theta_f]$, where i and f

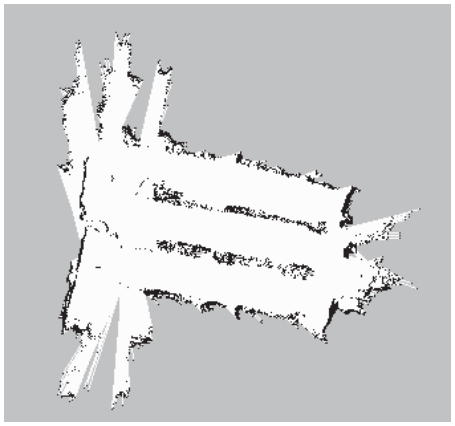

Fig. 5: Occupancy grid map generated by RTAB-MAP

Fig. 6: Greenhouse environment

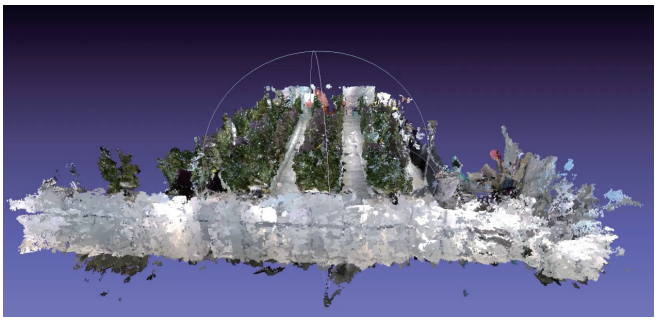

Fig. 8: 3D point cloud of environment

indicating the initial and final positions. The path planning algorithms can be divided into two broad categories:

1) **Global path planning**: When the environment is completely known before the robot moves, a collision-free trajectory with the lowest cost from the starting point to the target can be obtained by global path planning algorithms, as well as the cost in terms of travelled distance, obstacle avoidance, time to completion, etc. In such cases, the complete information can only be available in static environments, where collision-free paths are selected and planned off-line. In this study we evaluated the RRT* and A* based global path planing.
2) **Local path planning**: Local path planning algorithms transform a path into suitable subpaths and the local planner creates the path taking into consideration the dynamic obstacle and the robot kinematics. And therefore, to recalculate the path at a specific update rate, the map is reduced to the surroundings of the robot called local map and is updated as the robot is moving around in the environment. It is not possible to use the whole map because the sensors are unable to update the map in all regions and a large number of cells would raise the computational cost. Therefore, with the updated local map and the global waypoints, the local planning generates avoidance strategies for dynamic obstacles and tries to match the trajectory as much as possible to the provided waypoints from the global planner.

Fig. 7: Occupancy grid map generated by RTAB-Map

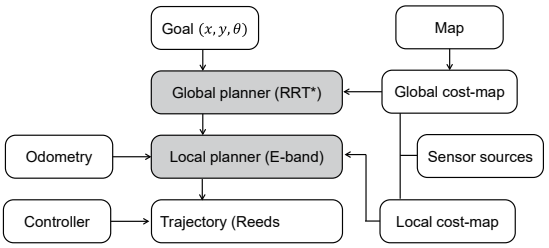

Fig. 9: Information flow among modules for navigation

The grid map is also broadly divided into two category of global cost map and local cost map. The cost map represents the cost values of the occupied cells which decrease with distance.

A. The implemented path planning method considering nonholonomic constraint for narrow pathways

The process of planning is explained in Figure 9. The path planning is based on the ROS navigation stack. After a goal is assigned as (x_f, y_f, θ_f), in the first step, RRT* algorithm generates a global trajectory considering the kinematic constraints of the mobile robot with nonholonomic constraint. In the next step, the E-band local planner [16] generates sub-trajectory by connecting the center points of the band using various heuristics. The sub-goal is passed to Reeds-Shepp curve, which generates the curve with the combination of curve and straight line to the sub-goal given by E-band planner. E-band planner drives the mobile robot towards the trajectory generated by Reeds-Shepp curve.

B. RRT based global planner*

Rapidly Random Tree generates a tree to reach the goal position by generating random nodes in the free space. The tree starts from the start node and expands until it reaches the target position (node). Figure 10 illustrates the path generated by the RRT* algorithm in the 3D space (x, y, θ) .

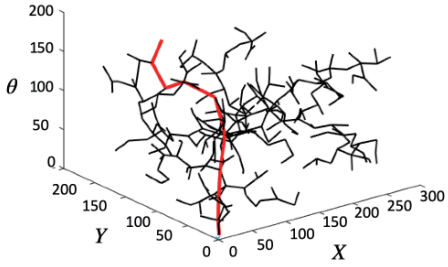

Fig. 10: Illustration of path planned by RRT*

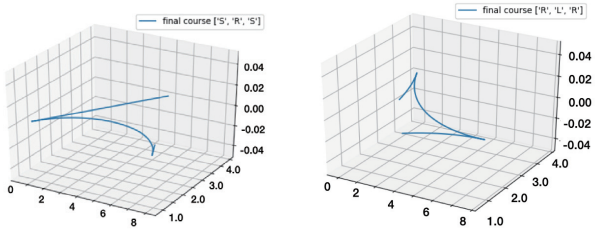

(a) (b)

Fig. 11: Illustrations of path planned by Reeds-Shepp

C. Reeds-Shepp curve

Reeds-Shepp's model is implemented to get a path for the mobile robot to navigate in the forwards and backwards direction. Reeds-Shepp curve is categorized into 12 classes, and admit a total of 48 patterns [11] of continuous curvature. A sub-trajectory of length P given by E-band local planner is mapping from start position in the configuration space C in 3D space, $\mathbb{R}^3$. The configuration is denoted by $\mathbb{R}3 = [x(s), y(s), \theta(s)]$, where $s \in [0, l]$ and l is the total length of P. Intuitively, P is a continuous curve in C. Given an initial configuration Q_i and a finial configuration Q_f, a path P is said to be feasible if $P(0) = Q_i$ and $P(l) = Q_f$ can be followed by the non-holonomic mobile robot. The two different generated path from the robot's current position and orientation, (x_r, y_r, θ_r), at any position s, is illustrated in Figure 11.

D. Evaluation of performance and discussion

For comparison, we evaluated two global path planners (RRT* and A*) and two local planners (E-band Reeds-Shepp and DWA). The distance of goal from start position was 8 m. Since RRT* algorithm uses sampling based approaches, it is not the deterministic and therefore sometime it failed to generate trajectory. The observed probability of generating trajectory using RRT* in narrow pathways environment was 80%. The averages computational evaluation is shown in TABLE V [4]. The execution time of the RRT* compared with A* is almost same, A* performed slightly slower. The DWA-based local planner shows poor performance to generate transversable trajectory in narrow pathways. The observed probability of generating trajectory using DWA in narrow pathways environment is 30%. On the other hand, the proposed combination of A*-based global planner and Reeds-Shepp curve-based local planner through E-band planner was also evaluated. The success rate of the method is 80%. In addition, the distance traveled (trajectory) by robot to reach goal position, RRT* generates an 10% shorter path than A*. The evaluation is done by kepping A* as global planner for DWA and Reeds sheep local planner.

[4]The abbreviation of above mentioned terms are S: Succeed to generate trajectory, T: Total trail.

TABLE V: Performance of path planning

Average path planning 20 trail (RRT*) Global planner		
Processing(s)	Path length(m)	Trail (S/T)
0.0980	7.20 m	18/20
Average path planning 20 trail (A*) Global Planner		
Processing(s)	Path length(m)	Trail (S/T)
0.1021	8.00 m	20/20
Average path planning 20 trail (E-band) - Local Planner		
Processing(s)	Path length(m)	Trail (S/T)
0.0821	9.6 m	6/20
Average path planning 20 trail (Reeds-Shepp) - Local Planner		
Processing(s)	Path length(m)	Trail (S/T)
0.0640	8.4 m	18/20

V. Discussion

This study focused on the analysis of mapping and path planning for a non-holonomic mobile robot in the narrow pathways and the factor on which it is evaluated are:

- The distance of mobile robot from the obstacles.
- The feasibility of path in the given environment for non-holonomic mobile robot.
- The computational time for path planning.
- Probability to generate feasible path.

When the non-holonomic mobile robot navigated through the curve, the Reeds-Shepp curve generated curve combining forward and reverse path planning. The mobile robot made switchback motions following the generated curves. Figures 12 and 13 show the trajectory generated by the mobile robot in two different environments.
The local path planner, E-band planner generated the sub-goal and Reeds-Shepp curve generated the trajectory, the trajectory generated by Reeds-Shepp curve is shown in Figure 14. Figure 15 illustrates the trajectory snapshot of mobile robot navigation in green-house environment.

VI. Conclusion

In this paper, we compared several path planning and mapping techniques. The experimental evaluation showed that in the fixed rack environment, G-mapping based mapping method using laser sensors and depth camera generates high quality occupancy grid map. In complex environment pathways surrounded by vegetable such as tomato plants, RTAB map generated reliable map for navigation. The path planning based on A* and Reeds- Shepp curve generated smother paths in low computational time. The combination of Reeds-Shepp curve and RRT* realized navigation through

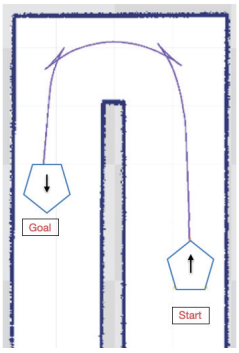

Fig. 12: Trajectory generated in narrow pathways (1)

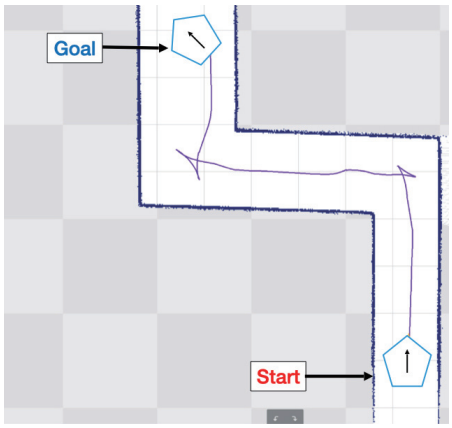

Fig. 13: Trajectory generated in narrow pathways (2)

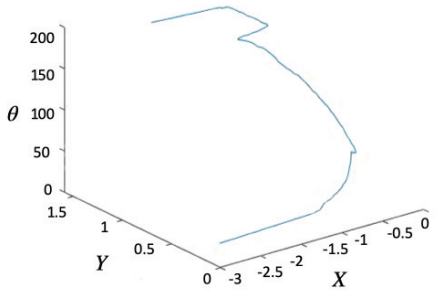

Fig. 14: Reeds-Shepp curve (trajectory) in 3D space (x, y, θ)

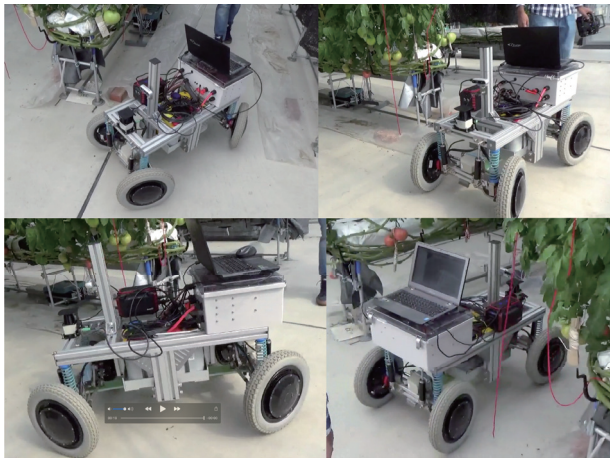

Fig. 15: Mobile robot navigation in green-house

narrow pathways by switch-back motion effectively, but there were some cases where environments are still more complex (*e.g.*, zig-zag narrow. The main future work is to improve the recovery behavior, in order to restart the planning if the robot is stuck or the behavior is too oscillatory. The connectivity of Reeds-Shepp based local planner can be improved in order to generate smother trajectory. Additionally, the navigation will be further tested in uneven terrain environment where vibration cost should be also taken into consideration [17].

ACKNOWLEDGMENTS

We would like to thank Mr. Suguru Yamane and Mr. Eiichi Makita of Shizuoka Prefectural Institute of Agriculture and Forestry for their great support, including the provision of experimental environments and advice. This work was partly supported by Artificial Research Promotion Foundation.

REFERENCES

[1] D. Kiss and D. Papp, Effective navigation in narrow areas: A planning method for autonomous cars, Proc. of IEEE International Symposium on Applied Machine Intelligence and Informatics, pp. 423-430, 2017.
[2] S. M. LaValle, Planning algorithms, Cambridge University Press, 2006.
[3] N. Nakao,*et al.*, Path Planning and Traveling Control for Pesticide-Spraying Robot in Greenhouse, Journal of Signal Processing, Vol. 21, No. 4, pp. 175-178, 2017.
[4] S. Tiwari *et al.*, Approach for Autonomous Robot Navigation in Greenhouse Environment for Integrated Pest Management, Proc. of IEEE/ION Position, Location and Navigation Symposium, pp. 1286-1294, 2020.
[5] J. J. Roldán, *et al.*, Heterogeneous Multi-Robot System for Mapping Environmental Variables of Greenhouses, Sensors, Vol. 16, No. 1018, 2016.
[6] G. Grisetti, C. Stachniss and W. Burgard, Improved Techniques for Grid Mapping With Rao-Blackwellized Particle Filters, IEEE Transactions on Robotics, vol. 23, no. 1, pp. 34-46, 2007.
[7] `http://wiki.ros.org/gmapping`
[8] M. Labbé and F. Michaud, RTAB-Map as an Open-Source Lidar and Visual SLAM Library for Large-Scale and Long-Term Online Operation, Journal of Field Robotics, Vol. 36, No. 2, pp. 416–446, 2019.
[9] R. Bohlin and L. E. Kavraki, Path planning using lazy PRM, Proc. of IEEE International Conference on Robotics and Automation, pp. 521-528, 2000.
[10] V. Vonásek, et al., RRT-path – A Guided Rapidly Exploring Random Tree, In: Kozłowski K.R. (eds) Robot Motion and Control 2009, Lecture Notes in Control and Information Sciences, vol 396, Springer.
[11] J. A. Reeds, L. A. Shepp, Optimal paths for a car that goes both forwards and backwards, Pacific Journal of Mathematics, Vol. 145, No. 2, pp. 367-393, 1990.
[12] L. Han, Q. H. Do and S. Mita, Unified path planner for parking an autonomous vehicle based on RRT, Proc. of IEEE International Conference on Robotics and Automation, pp. 5622-5627, 2011.
[13] `https://github.com/gkouros/reeds-shepp-paths-ros`
[14] M. Labbé and F. Michaud, Online global loop closure detection for large-scale multi-session graph-based SLAM, Proc. of IEEE/RSJ International Conference on Intelligent Robots and Systems, pp. 2661-2666, 2014.
[15] `http://wiki.ros.org/move_base`
[16] S. Quinlan and O. Khatib, Elastic bands: connecting path planning and control, Proc. of IEEE International Conference on Robotics and Automation, Vol.2, pp. 802-807, 1993.
[17] M. A. Bekhti and Y. Kobayashi, Regressed Terrain Traversability Cost for Autonomous Navigation Based on Image Textures, Applied Sciences, Vol. 10, No. 1195, 2020.